

ACCEPTED MANUSCRIPT

Investigations of the gate-instability characteristics in Schottky/ohmic type p-GaN gate normally-off AlGaIn/GaN HEMTs

To cite this article before publication: Changkun Zeng *et al* 2019 *Appl. Phys. Express* in press <https://doi.org/10.7567/1882-0786/ab52cc>

Manuscript version: Accepted Manuscript

Accepted Manuscript is “the version of the article accepted for publication including all changes made as a result of the peer review process, and which may also include the addition to the article by IOP Publishing of a header, an article ID, a cover sheet and/or an ‘Accepted Manuscript’ watermark, but excluding any other editing, typesetting or other changes made by IOP Publishing and/or its licensors”

This Accepted Manuscript is © 2019 The Japan Society of Applied Physics.

During the embargo period (the 12 month period from the publication of the Version of Record of this article), the Accepted Manuscript is fully protected by copyright and cannot be reused or reposted elsewhere.

As the Version of Record of this article is going to be / has been published on a subscription basis, this Accepted Manuscript is available for reuse under a CC BY-NC-ND 3.0 licence after the 12 month embargo period.

After the embargo period, everyone is permitted to use copy and redistribute this article for non-commercial purposes only, provided that they adhere to all the terms of the licence <https://creativecommons.org/licenses/by-nc-nd/3.0>

Although reasonable endeavours have been taken to obtain all necessary permissions from third parties to include their copyrighted content within this article, their full citation and copyright line may not be present in this Accepted Manuscript version. Before using any content from this article, please refer to the Version of Record on IOPscience once published for full citation and copyright details, as permissions will likely be required. All third party content is fully copyright protected, unless specifically stated otherwise in the figure caption in the Version of Record.

View the [article online](#) for updates and enhancements.

Investigations of the gate-instability characteristics in Schottky/ohmic type p-GaN gate normally-off AlGaIn/GaN HEMTs

Changkun Zeng¹, Weizong Xu^{1*}, Yuanyang Xia², Danfeng Pan¹, Yiwang Wang¹, Qiang Wang², Youhua Zhu^{2,3}, Fangfang Ren¹, Dong Zhou¹, Jiandong Ye¹, Dunjun Chen¹, Rong Zhang¹, Youdou Zheng¹, and Hai Lu^{1*}

¹ School of Electronic Science and Engineering, Nanjing University, Nanjing 210093, China.

² CorEnergy Semiconductor Co. Ltd., Suzhou 215600, China

³ School of Electronics and Information, Nantong University, Nantong 226019, China

E-mail: wz.xu@nju.edu.cn, hailu@nju.edu.cn

In this work, the impacts of Schottky- and ohmic-type gate contacts on devices stability of p-GaN gate AlGaIn/GaN high electron mobility transistors were experimentally investigated. In the Schottky-gate devices, drastic gate instability were observed under positive gate bias and elevated temperatures, featuring evident negative threshold voltage shift especially at low gate voltage region. By contrast, ohmic-gate devices exhibit superior gate stability with near-zero threshold voltage shift. Correspondingly, a physics picture of hole injection/emission processes in the p-GaN layer was established for the understanding of the distinct gate stability behaviors with different gate contact types.

1
2
3 Normally-off AlGaIn/GaN high electron mobility transistors (HEMTs) have received
4 increasing demands in power applications for their fail-safe operation capability and
5 simple gate drive configuration.¹⁻²⁾ Among the approaches to realize intrinsic normally-off
6 operation, p-GaN gate technology, which employs a p-GaN cap layer to deplete the
7 2-dimensional electron gas (2DEG) channel, has dominated the scene of
8 commercialization owing to its lower parasitic inductance and advantageous $R_{ON} \cdot Q_G$ figure
9 of merit.³⁻⁴⁾ Meanwhile, high speed and high efficiency GaN power integrated circuits
10 based on p-GaN gate power HEMTs have also been demonstrated in recent years.⁵⁻⁶⁾

11
12
13
14
15
16
17
18
19 The gate structure of metal/p-GaN/AlGaIn/GaN consists of a hetero p-i-n junction and a
20 metal/p-GaN junction of either Schottky or ohmic type.⁷⁻⁸⁾ As compared to an ohmic-type
21 gate, the Schottky gate contact features lower gate leakage current and larger gate driving
22 margin, given that the metal/p-GaN Schottky junction is reverse biased at a forward gate
23 bias.^{4,9-10)} However, due to the poor blocking capability of the Schottky junction on the Mg
24 doped p-GaN layer,¹¹⁻¹³⁾ hole injection occurs under the forward gate bias.¹³⁻¹⁴⁾ These extra
25 holes in the gate stacks could then cause unfavorable gate instability issues.^{8,15-16)} The
26 resultant threshold voltage (V_{th}) shift may induce unintentional operation point drift of the
27 device that causes extra power conversion efficiency loss or gate degradation.¹⁷⁻²⁰⁾
28
29
30
31
32
33
34
35
36
37
38
39
40
41
42
43 Therefore, to further optimize the gate contact structure for the p-GaN gate normally-off
44 AlGaIn/GaN HEMT, it is of particular interest to make clear the gate stability
45 characteristics and to clarify the underlying physical mechanism of possible gate instability
46 for both Schottky/ohmic-type gated devices.

47
48
49
50
51
52
53
54
55
56
57
58
59
60
In this work, p-GaN gate AlGaIn/GaN HEMTs utilizing both Schottky and ohmic type
gate contacts were demonstrated with their unique gate stability performances revealed. It
was found that, Schottky-type p-GaN gate HEMT encounters evident gate instability under
positive gate bias and elevated temperatures. And the shift of threshold voltage tends to be
much higher in low gate voltage (V_{GS}) region, i.e. V_{GS} from 0 V to 3 V. A physics model of
hole injection and accumulation in the floating p-GaN layer was established to understand
these unique gate stability behaviors. In contrast, ohmic-type device exhibits excellent gate
stability against gate bias and operation temperatures, which should be attributed to the
conductive gate contact that effectively alleviates the hole accumulation effect.

1
2
3 Fig. 1(a) illustrates the cross-sectional schematic of the p-GaN gated AlGaIn/GaN
4 HEMTs. The epitaxial layer was grown by metal organic chemical vapor deposition
5 (MOCVD) on a 6-inch commercial Si substrate. It consists of a 4.6- μm GaN buffer layer, a
6 300-nm GaN channel layer, a 1-nm AlN space layer, a 20-nm Al_{0.17}Ga_{0.83}N barrier layer,
7 and a 100-nm Mg-doped p-GaN cap layer. The Mg atom concentration in the p-GaN cap
8 layer is $2 \times 10^{19} \text{ cm}^{-3}$, and the hole density was measured to be $4.5 \times 10^{17} \text{ cm}^{-3}$ by Hall
9 measurements.
10

11
12
13
14
15
16
17 In the device fabrication processes, device isolation was firstly performed with nitrogen
18 ion implantation. Then, inductively coupled plasma (ICP) dry etching was utilized to etch
19 the p-GaN in the ohmic region, and was followed by the treatment with
20 Tetramethylammonium Hydroxide (TMAH) solution to remove the etching-related
21 damages. Subsequently, metal stack of Ti/Al/Ni/Au (40/80/40/100 nm) was deposited for
22 ohmic drain/source formation. Two types of gate contact for p-GaN gate HEMTs have
23 been fabricated, i.e. Schottky and ohmic. Both contacts were made of Ni/Au (20/20 nm),
24 while an extra 5-min post-annealing process at 550 °C in air (N₂:O₂ = 4:1) has been
25 performed for the ohmic gate contact formation.²¹⁻²² Fig. 1(b) illustrates the gate-to-gate
26 *I-V* characteristics of both two types of gate contacts. The annealed gate contacts present
27 near ohmic performance (red curve) and much higher current level in comparison to the
28 as-deposited Schottky-type gate contacts (blue curve).
29
30
31
32
33
34
35
36
37
38
39

40
41 Static electrical characterization was firstly performed on the Schottky type gate contact
42 devices with devices geometries of $L_{GS}=6\mu\text{m}$, $L_G/W_G=4\mu\text{m}/90\mu\text{m}$, $L_{GD}=15\mu\text{m}$. Fig. 1(c)
43 presents the transfer gate leakage characteristics of the fabricated devices with a drain
44 voltage (V_{DS}) of 0.5 V. The fabricated AlGaIn/GaN HEMT exhibits a V_{th} of ~ 1.5 V by linear
45 extraction, an on-to-off ratio up to 1×10^7 (red curves), a subthreshold swing (SS) of ~ 197
46 mV/dec, revealing the normally-off operation mode with excellent gate controllability.
47
48
49
50

51
52 Bi-directional *I-V* measurements were subsequently performed to evaluate the devices
53 gate stability performances. As shown in Fig. 2(a), evident hysteresis in the transfer
54 characteristics could be observed, featuring an elevated drain current (I_D) and negative V_{th}
55 shift (ΔV_{th}) in the backward measuring curve. Fig. 2(b) plots the *I-V* characteristics of
56 bi-directional measurements with various maximum forward gate bias (V_{GS_max}). With an
57
58
59
60

1
2
3 increasing V_{GS_max} , higher I_D and larger ΔV_{th} could be observed in the range of $0V <$
4 $V_{GS_max} < 3V$. This has revealed the dominance of positive gate bias in generating the
5 observed gate instability. However, it should be noted that as the V_{GS_max} extends 3 V, ΔV_{th}
6 and I_D exhibits saturation in the backward measurement.

7
8
9
10
11 These distinct behaviors observed in the bi-directional measurements should be
12 attributed to the charge storage in the floating p-GaN layer.²³⁻²⁴⁾ Fig. 3 illustrates the energy
13 band diagram of the gate stack of the p-GaN gate HEMT under different gate bias
14 conditions. With a relatively low gate bias ($0V < V_{GS} < 3V$), the holes could be injected
15 from the gate metal to the p-GaN layer either by tunneling through the Schottky junction
16 barrier or by thermal emission, i.e. process (i) as illustrated in Fig. 3(a). Meanwhile, due to
17 the band offset between the valence bands of p-GaN and AlGaIn, the injected holes would
18 accumulate at the p-GaN/AlGaIn interface without leaking through the AlGaIn barrier.
19 Then, the p-GaN layer turns into a floating layer with extra positive charges, inducing
20 downward band bending of gate stack and enhancing the accumulation of electrons in the
21 2DEG channel. Resultantly, increasing of I_D and negative shift of V_{th} could be observed.
22 Under a higher gate bias (e.g., $V_G > 3 V$), the overall band bending of the hetero p-i-n
23 junction would lead both the conduction and valence band of p-GaN layer become lower
24 than that of the GaN channel, as illustrated in Fig. 3(b). Consequently, processes of 2DEG
25 electrons spilling over the AlGaIn barrier and pumping out of holes from p-GaN/AlGaIn
26 interface to the GaN channel would be triggered,²⁵⁾ contributing to a sharp increase of gate
27 leakage. This was verified by the measured I_G characteristics at $V_{GS} > 3 V$, as presented in
28 Fig. 1(c). Both these two processes would counteract the holes accumulation at
29 p-GaN/AlGaIn interface either by electron-holes recombination or by directly pumping out
30 the holes, in spite of enhanced hole injection from the gate metal at higher forward gate
31 bias.⁸⁾ Ultimately, gate instability as a result of extra holes accumulated at p-GaN/AlGaIn
32 interface would be alleviated, as shown in Fig. 2.

33
34
35
36
37
38
39
40
41
42
43
44
45
46
47
48
49
50
51
52
53
54
55
56
57
58
59
60
In the backward measurement, as the gate bias drops to near zero in the backward I - V
measurement, i.e. the knee point B in Fig. 2(a), the blocking effect of Schottky junction
barrier on the accumulated holes reduces. This would facilitate the release of holes from
the p-GaN/AlGaIn interface to gate metal, i.e. process (iv) as illustrated in Fig. 3(c). The

1
2
3 gate-bias-driving removal of the extra holes in the gate stack would contribute an extra
4 negative variation of V_{GS} (ΔV_{GS}), resulting in a reduced SS .²⁶⁾ This process was verified by
5 the sub-60mV/dec SS , i.e. 54 mV/dec, being apparently lower than those of previously
6 reported p-GaN gate AlGaIn/GaN HEMTs.²⁷⁻²⁸⁾

7
8
9 Presented in Fig. 4 are the temperature dependent transfer curves from bi-directional
10 measurements. As temperature increased from 25 °C to 125 °C, V_{th} shifted negatively in
11 the forward measurements, thus temperature dependent gate instability was verified. This
12 could be explained by the enhanced hole injection from the gate metal to the floating
13 p-GaN layer via thermal assisted emissions. The resultant larger number of accumulated
14 holes from the gate metal would induce higher positive charging effect in the gate stack
15 and thus lead to lower V_{th} . It could be noted that the on-state I_{DS} drops with the elevated
16 temperature, which should be a result of the mobility degradation in the 2DEG channel,
17 being verified by the power law exponents of ~ -2.1 in the log-log fittings between I_D and
18 the temperature at $V_{GS} = 5$ V.²⁹⁻³¹⁾ The difference from the expected value of -1.5 for pure
19 mobility degradation should be related to the temperature dependence of the access
20 resistance.

21
22
23 As temperature went higher, processes of channel electrons spilling over the AlGaIn
24 barrier and holes injection into the GaN channel layer would be intensified and occur at
25 lower gate bias. The negative shift in turning on voltage of I_G and point A at higher
26 temperatures has validated this physics picture. On the other hand, only slight temperature
27 dependence could be observed in the reverse measuring curve. This corresponds well with
28 the physics model presented in Fig. 3(c), where the pumping of accumulated holes from
29 p-GaN to the gate metal as gate bias dropped to negative should be dominated by the
30 electric-field induced depletion, instead of thermal emission. In general, Schottky type
31 p-GaN gate AlGaIn/GaN HEMT is facing with serious intrinsic gate stability issues, being
32 highly sensitive to forward gate bias (especially in low voltage range) and operation
33 temperature.

34
35
36 As a comparison, transfer and gate stability characteristics of ohmic-type p-GaN gate
37 AlGaIn/GaN HEMT have been evaluated with results presented in Fig. 5(a), where a
38 comparatively lower V_{th} of ~ 0.35 V is exhibited. And in the bi-directional measurements,
39
40
41
42
43
44
45
46
47
48
49
50
51
52
53
54
55
56
57
58
59
60

1
2
3 nearly zero hysteresis could be observed in the transfer characteristics, independent of
4 forward gate bias and measuring temperature. This should be attributed to the absence of
5 the floating p-GaN region between the Schottky junction barrier and the p-GaN/AlGaN
6 interface. Therefore, in terms of gate stability, ohmic-type p-GaN gate AlGaN/GaN HEMT
7 features more desirable gate stability against both gate forward bias and temperature.
8
9
10
11
12

13 In summary, this work has focused on the impacts of Schottky and ohmic gate contact
14 on gate stability performances of p-GaN gate AlGaN/GaN HEMTs. It was found that,
15 devices with Schottky-type gate contact are facing with serious intrinsic gate stability
16 issues, being sensitive to positive gate bias and operation temperatures, especially in low
17 positive gate bias region, while ohmic-gate devices exhibited excellent stability against
18 gate bias and operation temperature. These findings are believed to provide substantial
19 knowledge for further optimizing the gate contact structure of p-GaN gate AlGaN/GaN
20 HEMTs, e.g. a hybrid combination of Schottky and ohmic gate contact structure might be
21 promising in obtaining the balance between gate control capability and stability in the
22 power applications.
23
24
25
26
27
28
29
30
31
32

33 **Acknowledgement**

34 This work was supported by the National Key R&D Program of China (No.
35 2017YFB0403000).
36
37
38
39
40
41
42
43
44
45
46
47
48
49
50
51
52
53
54
55
56
57
58
59
60

References

- 1) H. Amano, Y. Baines, E. Beam, M. Borga, T. Bouchet, P. R. Chalker, M. Charles, K. J. Chen, N. Chowdhury, R. Chu, C. De Santi, M. M. De Souza, S. Decoutere, L. Di Cioccio, B. Eckardt, T. Egawa, P. Fay, J. J. Freedman, L. Guido, O. Häberlen, G. Haynes, T. Heckel, D. Hemakumara, P. Houston, J. Hu, M. Hua, Q. Huang, A. Huang, S. Jiang, H. Kawai, D. Kinzer, M. Kuball, A. Kumar, K. B. Lee, X. Li, D. Marcon, M. März, R. McCarthy, G. Meneghesso, M. Meneghini, E. Morvan, A. Nakajima, E. M. S. Narayanan, S. Oliver, T. Palacios, D. Piedra, M. Plissonnier, R. Reddy, M. Sun, I. Thayne, A. Torres, N. Trivellin, V. Unni, M. J. Uren, M. Van Hove, D. J. Wallis, J. Wang, J. Xie, S. Yagi, S. Yang, C. Youtsey, R. Yu, E. Zanoni, S. Zeltner, and Y. Zhang, *J. Phys. D, Appl. Phys.* **51**, 163001 (2018).
- 2) K. J. Chen, O. Häberlen, A. Lidow, C. Lin Tsai, T. Ueda, Y. Uemoto, and Y. Wu, *IEEE Transactions on Electron Devices* **64**, 779 (2017).
- 3) O. Hilt, F. Brunner, E. Cho, A. Knauer, E. Bahat-Treidel, and J. Würfl, *IEEE 23rd International Symposium on Power Semiconductor Devices and ICs* 239 (2011).
- 4) I. Hwang, J. Kim, H. S., Choi, H., Choi, J., Lee, K. Y. Kim, J. Park, J. C. Lee, J. Ha, J. Oh, J. Shin, and U. Chung, *IEEE Electron Device Letters* **34**, 202 (2013).
- 5) T. J. Flack, B. N. Pushpakaran, and S. B. Bayne, *Journal of Electronic Materials* **45**, 2673 (2016).
- 6) E. A. Jones, F. F. Wang, and D. Costinett, *IEEE Journal of Emerging and Selected Topics in Power Electronics* **4**, 707 (2016).
- 7) B. Li, H. Li, J. Wang, and X. Tang, *IEEE Electron Device Letters* **40**, 1389 (2019).
- 8) J. He, G. Tang, and K. J. Chen, *IEEE Electron Device Letters* **39**, 1576 (2018).
- 9) F. Lee, L. Y. Su, C. H. Wang, Y. R. Wu, and J. Huang, *IEEE Electron Device Letters* **36**, 232 (2015).
- 10) L. Efthymiou, G. Longobardi, G. Camuso, T. Chien, M. Chen, and F. Udrea, *Applied Physics Letters* **110**, 123502 (2017).
- 11) K. Shiojima, T. Sugahara, and S. Sakai, *Applied Physics Letters* **77**, 4353 (2000).
- 12) M. Tapajna, O. Hilt, E. Bahat-Treidel, J. Würfl, and J. Kuzmík, *IEEE Electron Device Letters* **37**, 385 (2016).
- 13) T. F. Chang, T. C. Hsiao, C. F. Huang, W. H. Kuo, S. F. Lin, G. S. Samudra, and Y. C.

- 1
2
3 Liang, IEEE Transactions on Electron Devices **62**, 339 (2014).
4
5 14) T. F. Chang, T. C. Hsiao, S. H. Huang, C. F. Huang, Y. H. Wang, G. S. Samudra, and Y. C.
6 Liang, IEEE 11th International Conference on Power Electronics and Drive Systems 681
7 (2015).
8
9 15) J. Wei, R. Xie, H. Xu, H. Wang, Y. Wang, M. Hua, K. Zhong, G. Tang, J. He, M. Zhang,
10 and K. J. Chen, IEEE Electron Device Letters **40**, 526 (2019).
11
12 16) H. Wang, J. Wei, R. Xie, C. Liu, G. Tang, and K. J. Chen, IEEE Trans. Power Electron.
13 **32**, 5539 (2017).
14
15 17) A. N. Tallarico, S. Stoffels, N. Posthuma, P. Magnone, D. Marcon, S. Decoutere, E.
16 Sangiorgi, and C. Fiegna, IEEE Transactions on Electron Devices **65**, 38 (2017).
17
18 18) I. Rossetto, M. Meneghini, F. Canato, M. Barbato, S. Stoffels, N. Posthuma, S. Decoutere,
19 A. N. Tallarico, G. Meneghesso, and E. Zanoni, Microelectronics Reliability **76**, 298
20 (2017).
21
22 19) E. Zanoni, M. Meneghini, G. Meneghesso, D. Bisi, I. Rossetto, and A. Stocco, IEEE 3rd
23 Workshop on Wide Bandgap Power Devices and Applications 75 (2015).
24
25 20) X. Li, G. Xie, C. Tang, and K. Sheng, Microelectronics Reliability **65**, 35 (2016).
26
27 21) J. Chen, W. D. Brewer, Advanced Electronic Materials **1**, 1500113 (2015).
28
29 22) B. Sarkar, P. Reddy, A. Klump, F. Kaess, R. Rounds, R. Kirste, S. Mita, E. Kohn, R.
30 Collazo, and Z. Sitar, Journal of Electronic Materials **47**, 305 (2018).
31
32 23) M. Ruzzarin, M. Meneghini, A. Barbato, V. Padovan, O. Haeberlen, M. Silvestri, T.
33 Detzel, G. Meneghesso, and E. Zanoni, IEEE Transactions on Electron Devices **65**, 2778
34 (2018).
35
36 24) A. Stockman, F. Masin, M. Meneghini, E. Zanoni, G. Meneghesso, B. Bakeroot, and P.
37 Moens, IEEE Transactions on Electron Devices **65**, 5365 (2018).
38
39 25) X. Tang, B. Li, H. A. Moghadam, P. Tanner, J. Han, and S. Dimitrijevic, IEEE Electron
40 Device Letters **39**, 1145 (2018).
41
42 26) Y. Shi, Q. Zhou, Q. Cheng, P. Wei, L. Zhu, D. Wei, A. Zhang, Wanjun Chen, and B.
43 Zhang, IEEE 30th International Symposium on Power Semiconductor Devices and ICs 96
44 (2018).
45
46 27) L. Y. Su, F. Lee, and J. J. Huang, IEEE Transactions on Electron Devices **61**, 460 (2014).
47
48
49
50
51
52
53
54
55
56
57
58
59
60

- 1
2
3 28) H. C. Chiu, Y. S. Chang, B. H. Li, H. C. Wang, H. L. Kao, C.W. Hu, and R. Xuan, IEEE
4 Journal of the Electron Devices Society **6**, 201 (2018).
5
6
7 29) W. Tan, M. Uren, P. Fry, P. Houston, R. Balmer , and T. Martin, Solid-State Electron **50**,
8 511 (2006).
9
10
11 30) R. Wang, Y. Cai, K. J. Chen, Solid-state Electronics **53**, 1 (2009).
12
13 31) O. Hilt, E. Bahat-Treidel, F. Brunner, A. Knauer, R. Zhytnytska, P. Kotara, and J. Wuerfl,
14 Journal of Physics: Conference Series **494**, 012001 (2014).
15
16
17
18
19
20
21
22
23
24
25
26
27
28
29
30
31
32
33
34
35
36
37
38
39
40
41
42
43
44
45
46
47
48
49
50
51
52
53
54
55
56
57
58
59
60

Accepted Manuscript

Figure Captions

Fig. 1. (a) Schematic cross-section image, (b) gate-to-gate I - V characteristics of both two types of gate contacts, (c) transfer and gate leakage characteristics at room temperature, of the p-GaN gate HEMT with Schottky-type gate contact.

Fig. 2. Transfer characteristics of p-GaN gate HEMT with Schottky-type gate contact in bi-directional measurements (a), and with different gate voltage sweeping range (b). The inset is the equivalent circuit of the p-GaN gate stack.

Fig. 3. Schematic band diagrams of the Schottky-metal/p-GaN/AlGaIn/GaN structure under different gate bias conditions. The physical processes of hole/electron injections and recombination are illustrated schematically.

Fig. 4. (a) Temperature dependent transfer characteristics of the p-GaN gate HEMT with Schottky gate contact in bi-directional measurements. (b) Log-to-log fits between drain current and temperatures.

Fig. 5. (a) Transfer and gate leakage characteristics, (b) temperature dependent transfer characteristics in bi-directional measurements, of the p-GaN gate HEMT with ohmic-type gate contact.

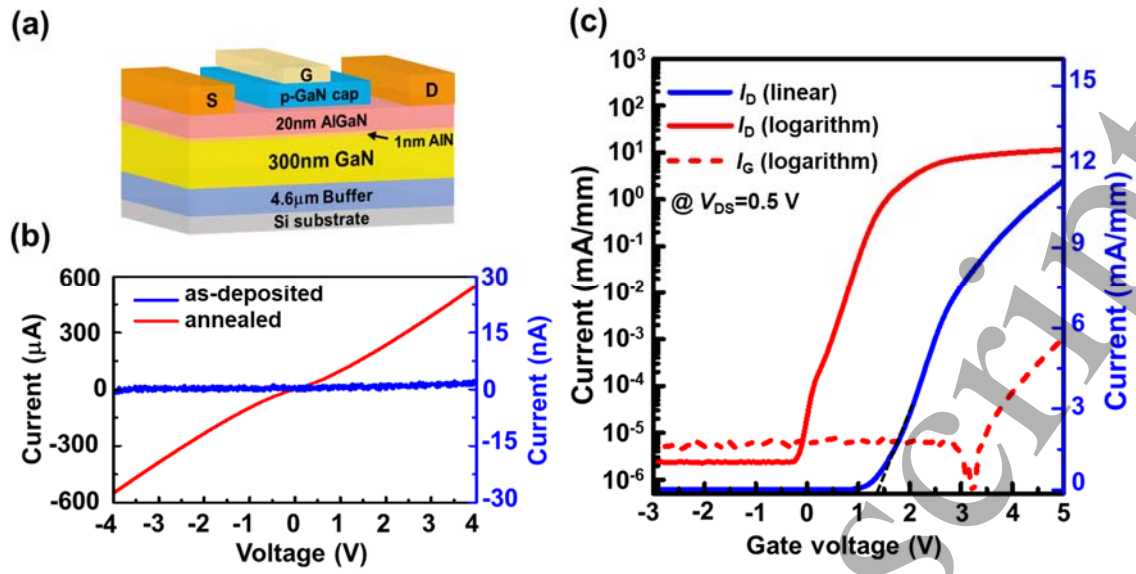


Fig. 1

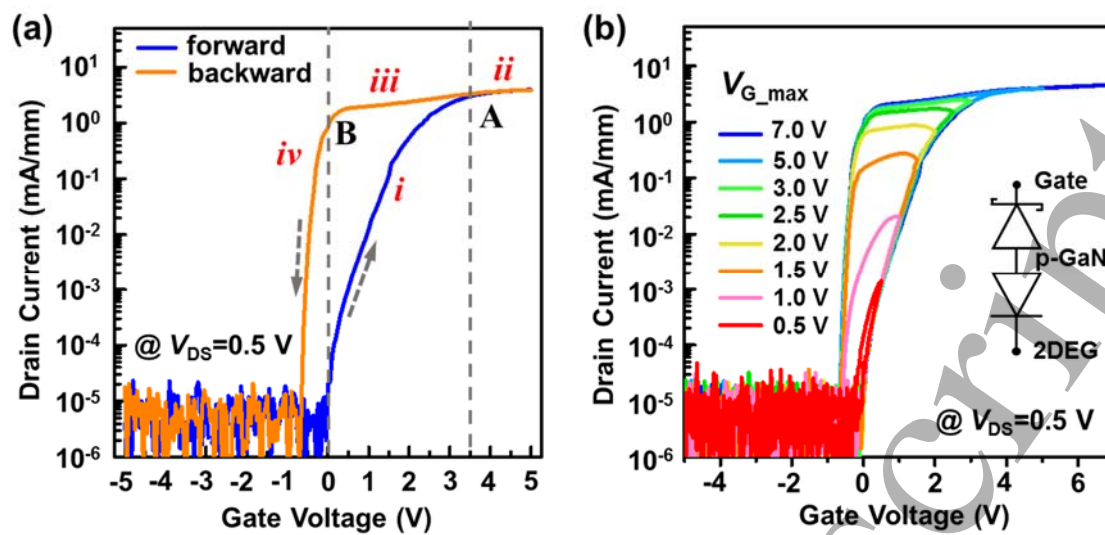


Fig. 2

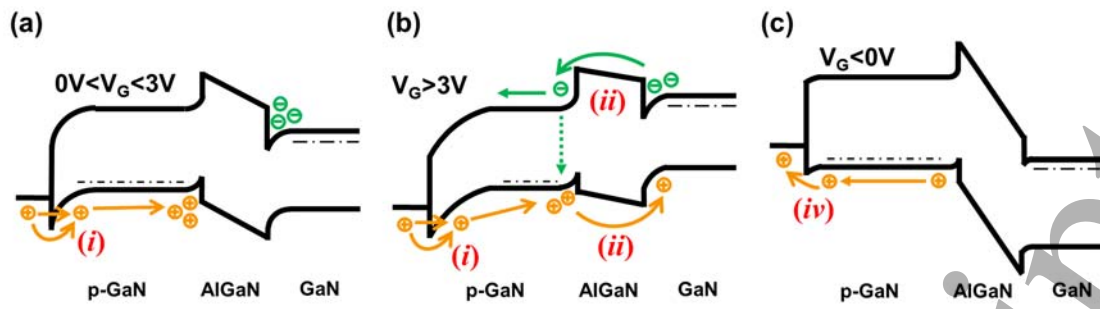


Fig. 3

Accepted Manuscript

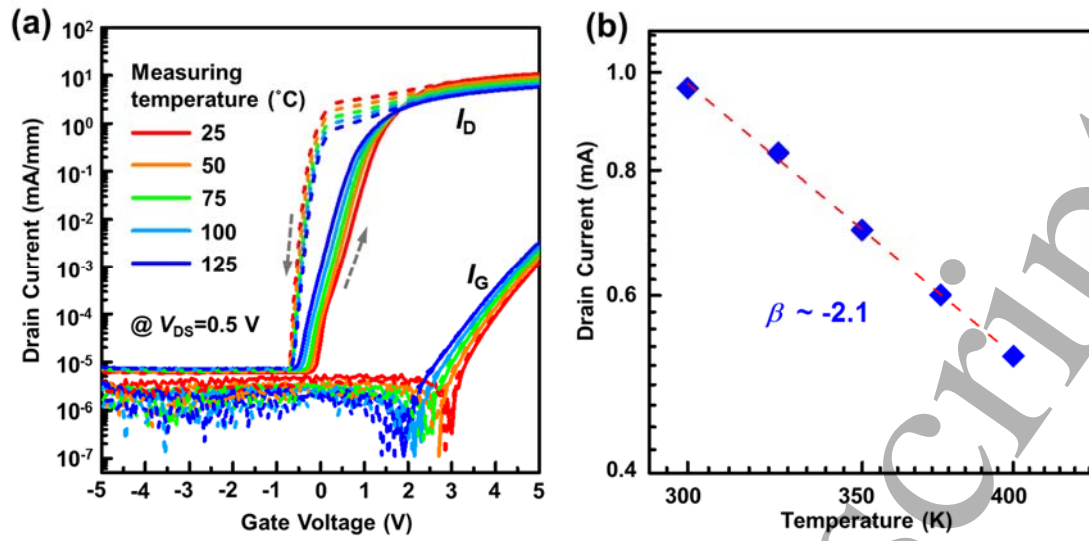


Fig. 4

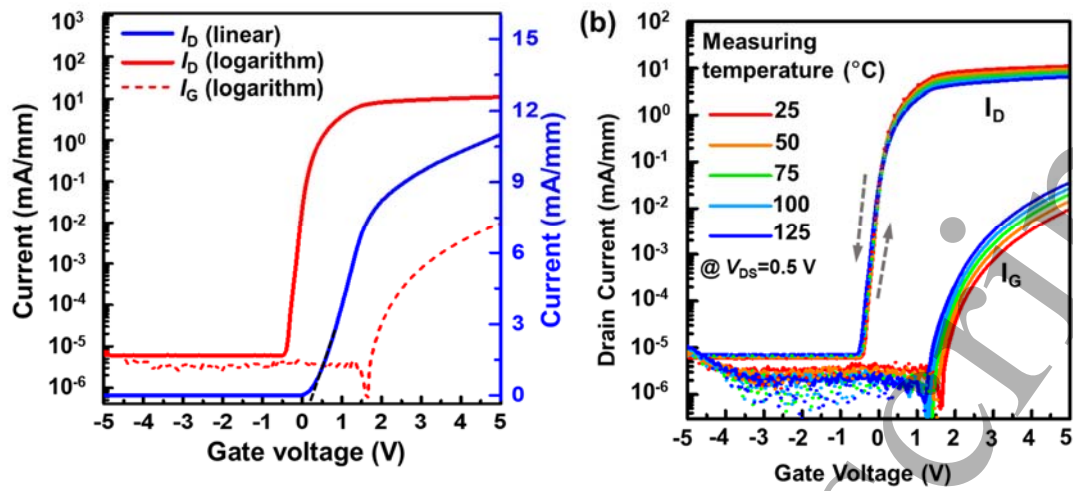


Fig. 5